Enhancing the Tensile Properties of Continuous Millimeter-Scale Carbon Nanotube Fibers by Densification

Frances A. Hill,*,[†] Timothy F. Havel,[‡] A. John Hart,[§] and Carol Livermore[||]

[†]Microsystems Technology Lab, Massachusetts Institute of Technology, 77 Massachusetts Ave., Cambridge, Massachusetts 02139, United States

[‡]Energy Compression Inc., Beverly, Massachusetts 01915, United States

[§]Department of Mechanical Engineering, Massachusetts Institute of Technology, 77 Massachusetts Ave., Cambridge, Massachusetts 02139, United States

[||]Department of Mechanical & Industrial Engineering, Northeastern University, 360 Huntington Avenue, Boston, Massachusetts 02115, United States

ABSTRACT: This work presents a study of the tensile mechanical properties of millimeter-long fibers comprising carbon nanotubes (CNTs). These CNT fibers are made of aligned, loosely packed parallel networks of CNTs that are grown in and harvested from CNT forests without drawing or spinning. Unlike typical CNT yarn, the present fibers contain a large fraction of CNTs that span the fibers' entire gauge length. The fibers are densified after growth and network formation to study how increasing the degree of interaction among CNTs in a network by various methods influences and limits the mechanical behavior of macroscopic CNT materials, particularly for the case in which the continuity of a large fraction of CNTs across the gauge length prevents failure purely by slip. Densification is carried out using various combinations of capillary-driven densification, mechanical pressure, and twisting. All methods of densification increase the fiber density and modify the nanoscale order of the CNTs. The highest strength and stiffness values (1.8 and 88.7 N tex^{-1}, respectively) are observed for capillary-densified fibers, whereas the highest toughness values (94 J g^{-1}) and maximum reversible energy density (1.35 kJ kg^{-1} or 677 kJ m^{-3}) are observed for fibers densified by mechanical pressure. The results suggest that the path to higher performance CNT materials may lie not only in the use of continuous and long CNTs but also in controlling their density and nanoscale ordering through modification of the as-grown networks, such as by capillary-driven densification.

KEYWORDS: *carbon nanotubes, fibers, tension, densification, energy storage*
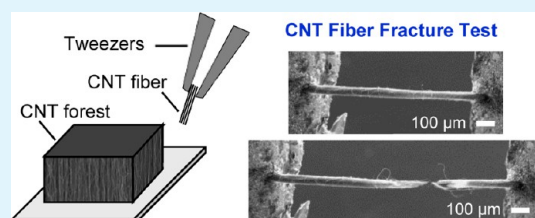
1. INTRODUCTION

The exceptional mechanical properties of carbon nanotubes (CNTs) make them a promising material for load-bearing applications ranging from aerospace laminates to body armor. To function as effective structural materials, the properties of large-scale CNT assemblies must closely match the properties of single defect-free CNTs, which have a Young's modulus of 1 TPa and strength on the order of 50−100 GPa.[1−3] To date, macroscale CNT materials, such as yarns and sheets, exhibit strength and stiffness values that fall far short of the properties of individual CNTs.[4,5] The reduction in performance of these hierarchical materials can be attributed to atomic defects in the CNTs, disorder of the CNT alignment, low packing density of the CNTs, spatial nonuniformities throughout the material, and nonideal inter-CNT load transfer that leads to slip.[6−9] An ideal macroscopic CNT fiber would be made from densely packed, long and high-quality CNTs and contain CNTs aligned along the axis of loading to provide maximum strength and stiffness. In contrast, SEM images of state of the art macroscopic CNT fibers and yarns show substantial amounts of CNT disorder on the nanoscale. Moreover, there is a lack of fundamental understanding of (i) how the densification of CNT fibers after growth modifies CNT organization and disorder and (ii) how individual CNT properties and CNT organization relate to fiber properties. To enable the manufacturing of CNT materials with superior performance, it is important to gain an understanding both of how densification controls CNT network organization and of how nonideal structure and organization influence and limit the mechanical behavior of macroscopic CNT materials.

This Article studies the mechanical properties of groupings of CNTs having millimeter-scale length in which a substantial fraction of the CNTs span the gauge length of the grouping; these groupings will hereafter be referred to as fibers. The fibers are distinct from CNT yarn because the fibers contain a large fraction of CNTs that we expect are continuous from one end of the gauge length to the other. In contrast, CNT yarn relies on overlaps between CNTs that are typically shorter than the
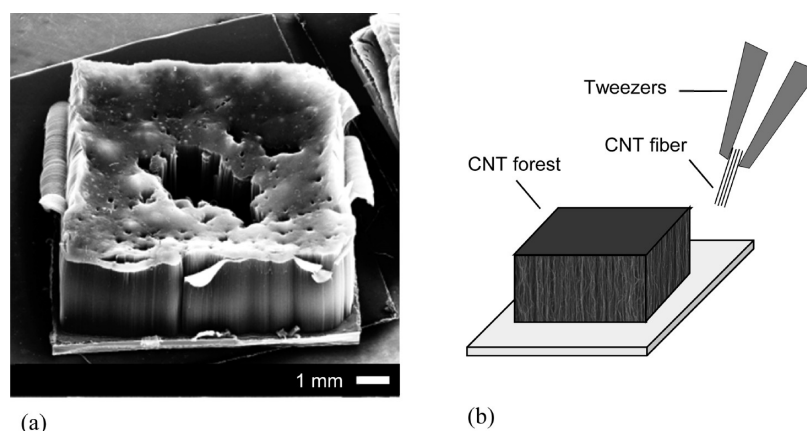
Figure 1. (a) SEM image of a CNT forest and (b) schematic diagram showing the mechanical separation of a small strand of CNTs from the side of a forest to form a fiber.

gauge length, and load bearing occurs via load transfer between overlapping CNTs. The primary failure mechanism of fibers is therefore expected to be the fracture of the covalent carbon bonds of the constituent CNTs compared with a combination of slip and fracture in yarns.

In other approaches, CNT yarns can be spun from the vapor phase in a chemical vapor deposition (CVD) reactor,[6] dry-spun from CVD-grown forests,[10,11] or wet-spun.[12,13] In yarn, tight packing of the largely parallel CNTs can establish strong intertube interactions to promote load transfer, whereas disordered packing can limit the load transfer as well as prevent the CNTs from being loaded uniformly. In studies of the performance of yarns, it is difficult to separate out the effects of load transfer among contacting CNTs (which can cause slip) from the effects of network structure, tangling, disorder, and impurities. From a scientific point of view, the value in studying the mechanical properties of the present fibers lies in the fact that a significant fraction of the constituent CNTs span the gauge length of the fiber so that slip plays less of a role in the fibers than in yarns. These millimeter-long fibers, therefore, serve as a simpler system in which to study the effects of CNT network structure and disorder on the load-bearing uniformity and mechanical properties of macroscopic assemblies of highly interacting CNTs, with the enhanced ability to vary one process parameter at a time and less dependence on the effects of slip. Conclusions from this work on fibers can in turn shed light on the physics governing the more complex behavior of CNT materials that rely on overlaps for structural cohesion, such as CNT yarns.

The CNTs used to create these fibers are grown in forests using CVD. Densification is a promising method to control fiber properties because as-grown CNT forests have low densities as compared, for example, with graphite, resulting in limited intertube interactions. Densification reduces a fiber's cross-sectional area and lowers the likelihood of geometry-induced uneven loading across the fiber, particularly for thick fibers. Additionally, there is an expectation that increasing the fiber density could enhance load transfer by increasing the contact area between CNTs, which should increase the fraction of CNTs that are load-bearing and therefore the fibers' mechanical strength and stiffness.

Enhancing the mechanical properties of CNT fibers is additionally important for mechanical energy storage.[14−18] Springs composed of dense, ordered assemblies of CNTs offer the potential to store energy with a density that matches the storage capabilities of electrochemical batteries and to release it quickly for high-power-density operation. The maximum energy density of ideal bundles of single walled carbon nanotubes (SWCNTs) loaded in tension along their axial direction is predicted to be 7.7×10^6 kJ m^{-3} or 5000 kJ kg^{-1} at 15% strain, which is three orders of magnitude higher than the energy density of steel springs[16,17] and compares favorably with the energy densities of electrochemical batteries (ranging from about 100 kJ kg^{-1} to 730 kJ kg^{-1}).[19] Exceptionally high reversible energy storage has previously been measured by compressing randomly oriented SWCNTs in powder form;[20] a potentially higher elastic energy density could be reached in CNTs loaded in tension rather than compression because the elastic loading of CNTs in tension is limited by only the elastic strain limit and not by the compressive buckling strain.[16] From an engineering perspective, high-performance macroscale CNT fibers could function as tensile springs with sufficient energy-storage levels to power microscale or milli-scale systems.

This study demonstrates how densification, using a range of techniques independently and in combination to modify the nanoscale order and density of the CNT network, can enhance the mechanical properties of CNT fibers under tension. To gain insight into the effects of network structure and disordered packing within fibers during loading and failure, tension tests to failure and tensile cyclic tests were performed on fibers densified using various combinations of capillary densification, mechanical pressure, and twisting. Additional tension tests were conducted using a deformation stage inside of a scanning electron microscope (SEM) to observe the behavior of fibers during loading and failure.

2. EXPERIMENTAL SECTION

CNT fibers of approximately 3 mm in length were created by mechanically separating small sections ("strands") from a 3 mm tall CNT forest (Figure 1a), as described in previous work.[17] Each strand contains millions of CNTs and was removed from the forest intact, without drawing or spinning (Figure 1b); as such, the overall length of a fiber is the same as the height of the forest. The forest was grown by thermal CVD from a thin-film catalyst on a silicon substrate.[21] The CNTs within the forest average 10 nm in outer diameter and have on average 4 to 5 walls. Although the CNTs are generally aligned along the vertical direction of the forest (parallel to the strand), the CNTs are tortuous because of intrinsic defects and their relatively low packing density (Figure 2). The average density of the CNT forest (and of the undensified fibers) is 17.6 kg m^{-3} (0.8% of the density of graphite). Fibers with different cross-sectional areas were prepared,
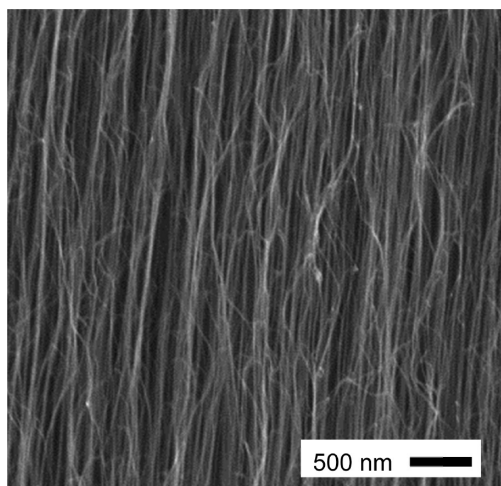
Figure 2. SEM image of the surface of an undensified fiber after placement in the test frame showing the alignment and general waviness of individual and bundled CNTs at a low packing density.

with areas ranging from 0.0011 to 0.11 mm^2, corresponding to a linear mass density range from 0.02 to 2 tex (1 tex = 1 mg m^{-1}). All of the fibers were prepared from the same forest to maximize the consistency of the starting material.

To examine how densification affects the fibers' mass density, structure, and mechanical properties, five sets of fibers were prepared. The densification factor and the corresponding fiber density after densification were obtained by measuring the average cross-sectional areas of fibers before and after densification with an optical microscope. The first set of fibers was not densified prior to testing. The second set of fibers was densified using capillary forces[22,23] by placing a drop of toluene onto each fiber and subsequently allowing the solvent to evaporate. The solvent draws the CNTs together as it leaves the fiber through evaporation and through wicking of the solvent into the porous surface on which the fiber is placed during the densification process. Fibers densified using this technique become sheetlike (Figure 3c), indicating that wicking into the underlying surface dominates over more axially symmetric evaporation in driving the elasto-capillary action between neighboring CNTs and bundles. A conservative estimate for the densification factor is 10; however, in some cases, the degree of densification varies along the fiber length. The densification factor of 10 is assumed for capillary-densified fibers for the remainder of the Article. The third set of fibers was densified mechanically by placing a fiber between two glass plates and sliding one plate over the other, perpendicular to the CNT orientation, so that the fiber adopted a tightly packed cylindrical shape. Measured densification factors between 3 and 83 were obtained using this technique, depending on the applied pressure and the linear mass density of the fiber. Higher applied pressures and larger fiber size both resulted in greater densification. The fourth set of fibers was prepared using mechanical densification (using the same method as the third set) followed by capillary densification. The fifth set of fibers was prepared by densifying fibers mechanically, mounting them on paper frames using epoxy, and then applying 720° twists to the fibers by rotating one frame relative to the other. Twisting was applied in an effort to increase the lateral pressure between CNTs, enhance inter-CNT friction, and increase load transfer. Figure 3 shows an undensified fiber (from set 1), a fiber densified using capillary effects that has become sheetlike (from set 2), and a mechanically densified fiber with a rounded cross section (from set 3). Each fiber was mounted on a testing frame, and images are shown both prior to and after a tension to failure test.

The fiber densities are plotted versus linear mass density in Figure 4. Capillary-driven densification resulted in densities of about 180 kg m^{-3} that are typically independent of fiber size; these densities are much lower than the typical densities of spun yarn, which are on the order of

1000 kg m^{-3}.[6,10,13,18,24] In contrast, the final densities of mechanically densified fibers depended on the fiber size. Mechanically densified fibers with linear mass densities greater than about 0.5 tex exhibited final densities on the order of 1000 kg m^{-3}, similar to spun yarns, with progressively smaller densities observed as the linear mass densities of mechanically densified fibers dropped below 0.5 tex. The fact that the final density depends on the fiber size for mechanically driven densification is an important finding for controlling fiber structure and properties. The fact that fiber size and fiber density are not fully independent parameters will also be relevant for interpreting the data relating the fibers' mechanical performance to their densities.

For tensile testing, the fibers were mounted onto thick paper frames using epoxy (Pacer Z-Poxy), as shown schematically in Figure 5. The fiber gauge length is 1.0 mm on average, with a standard deviation of 0.2 mm, across 133 fibers tested. To form the grips, 1 mm long sections at each of the two ends of the 3 mm long fibers were coated in epoxy, leaving on average a 1 mm long open region in the center of the fiber as the gauge length for tensile testing. Because the gauge length is limited to the center of the forest and not the regions of the early forest growth or growth termination, a substantial fraction of the CNTs may be assumed to span the gauge length as described earlier. This is supported by previous measurements of density as a function of the vertical position within forests made by the same CVD method.[25] The top of the forest forms a low-density "crust" in which many CNTs have not yet begun to grow. The peak number density of CNTs in the forest occurs at approximately one-third of the height, as measured from the top of the forest, corresponding to the start of the gauge length. The number density of CNTs then decays steadily with increasing depth into the forest until it reaches the threshold value at which growth terminates. Number densities from the previous study declined by less than a factor of 2 in the central third of the forest height,[25] indicating that approximately 50% of the CNTs in the present forests may be expected to be continuous across the gauge length. Although the use of gauge lengths comprising the center of the approximately 3 mm forest growth minimizes CNT discontinuity, it also limits the ability to study the effects of varying the gauge length over a wide range.

Tensile tests were conducted using an MTS Nano UTM Testing System with a 0.5 N load cell. A strain rate of 2×10^{-3} s^{-1} was used for tension tests to failure, and a strain rate of 3×10^{-3} s^{-1} was used for cyclic tensile testing. To record video of the fibers during loading and failure, a custom-built deformation stage was used inside of a large-chamber SEM. For these tests, fibers were mounted onto copper frames using a silver conductive epoxy (MG Chemicals 8331-14G).

One advantage of using epoxy to grip the ends of a fiber for tensile loading is that the epoxy infiltrates the cross-section of a fiber, thereby permitting direct loading of the CNTs throughout the fiber cross-section. Complete epoxy infiltration throughout the fiber cross sections was confirmed by cleaving the epoxy at the grips and examining the cross-section in an optical microscope (for the case of nonconductive epoxy) and in an SEM (for the case of conductive epoxy). The two epoxies were carefully chosen such that they penetrated the fiber at the grips but did not wet the fiber along its length, thereby leaving a clean region for tensile testing. Any deformation of the epoxy grips during tension tests would invalidate the strain measurements provided by the Nano UTM. Therefore, tests were conducted to evaluate deformation of the epoxy grips during loading by recording video images of the fibers and epoxy grips during tension tests. The video was analyzed using digital image correlation software (Vic2D) to obtain a second independent measure of the strain in the fibers. The strain data showed no detectable compliance in the epoxy grips, indicating that the forces in the fibers during tension tests were sufficiently small to neglect epoxy compliance in the strain data provided by the Nano UTM.

3. RESULTS AND DISCUSSION

Tension tests to failure were conducted on the five sets of fibers, representing a total of 133 fibers tested. Examples of the specific stress versus strain curves for undensified fibers are
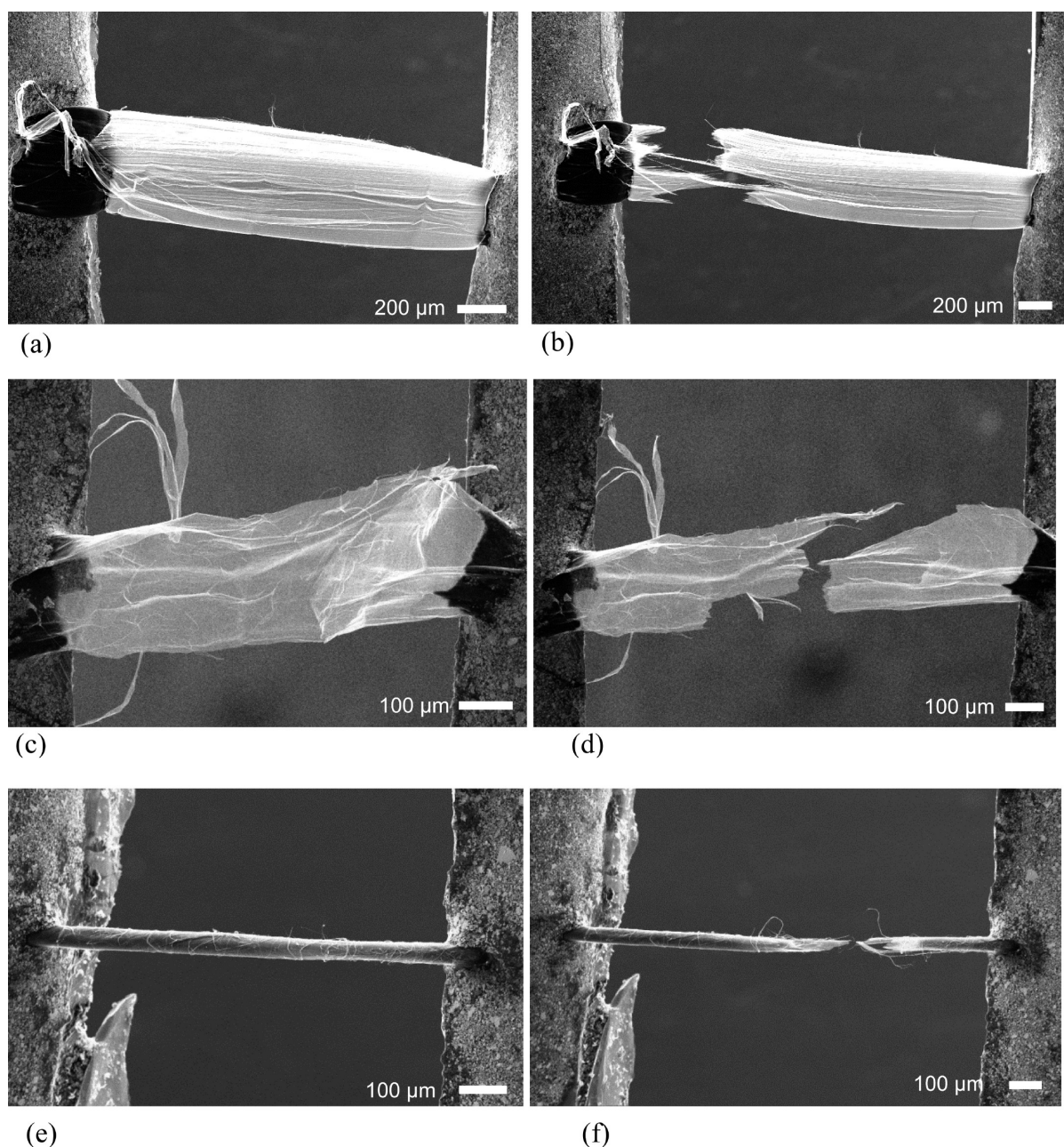
Figure 3. SEM images taken during in situ tensile tests of fibers mounted on a deformation stage before and after fracture that were densified using different techniques: (a,b) undensified, (c,d) capillary densified using toluene, and (e,f) mechanically densified.

plotted in Figure 6. Similar curve shapes were recorded for the four sets of densified fibers. The curves are nonlinear and typically exhibit a gradual increase in slope at low strains, with a highest slope at midstrain and a gradual or occasionally abrupt decrease in the slope at high strains. The gradual increase in slope at low strains suggests that the fraction of load-bearing CNTs gradually increases as slack is removed from the fiber. This observation, along with the typical lack of a linear loading region, indicates that spatial nonuniformities are present in the fibers and that load-bearing is nonuniform throughout the fiber. The slope is highest at moderate strain, which is when the largest relative fraction of CNTs is load bearing. The gradual decrease in slope at high strains occurs because fracture initiates in a localized region of a fiber that presumably carries a disproportionate amount of the load and then gradually propagates through the rest of the fiber. This behavior was

commonly observed in fibers loaded to failure in an SEM. The fibers fracture at strains between 5 and 12%, which is higher than what one would expect of single MWCNTs grown in a forest. Such a high failure strain is thought to be the result of the fiber nonuniformities as well as the tortuosity of the CNTs (each CNT is not taut at the start of a tension test because of its waviness) that increases the slack in the fiber. CNT tortuosity is expected to reduce fiber stiffness, and the atomic defects associated with the CNTs' tortuous nature are expected to lower the fiber strength.

The measured specific strength and specific stiffness values are plotted versus fiber linear mass density in Figure 7a–f. For fibers densified using all of the methods described above, there is a clear inverse relationship between the specific stiffness and linear mass density as well as between the specific strength and linear mass density, which was also observed in previous studies
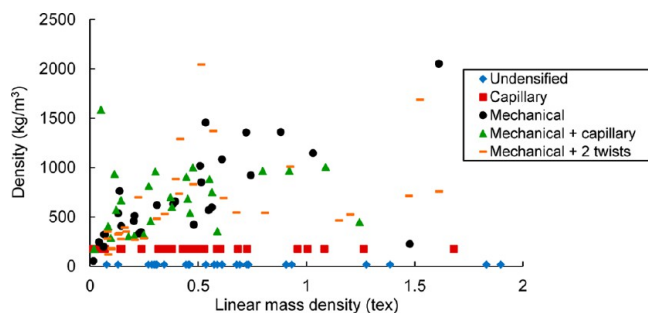
Figure 4. Scatter plot of the fiber density vs measured linear mass density for the fibers studied here. The values for capillary-densified fibers and undensified fibers are taken to be constant on the basis of measurements of fibers prepared by those methods. The densities of the fibers densified mechanically (with or without a secondary densification method) generally increase with the fibers' linear mass density.
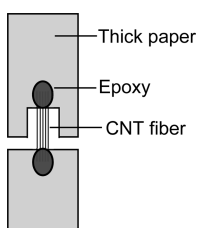

Figure 5. Schematic diagram of a fiber mounted onto a frame with epoxy for mechanical testing.
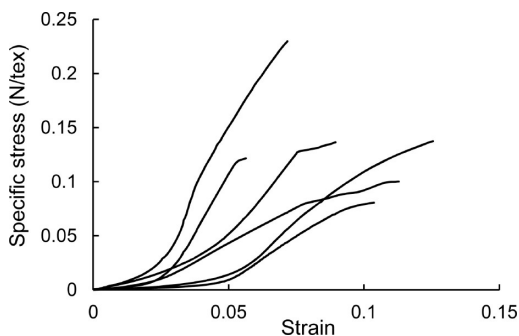

Figure 6. Typical specific stress vs strain curves for undensified fibers, with a morphology similar to the fiber shown in Figure 3a. The curves terminate at the point of failure.

by our own and other groups.[17,24,26] To establish that the observed dependence of strength and stiffness on linear mass density is not simply an effect of sampling bias (i.e., more samples were measured with smaller linear mass densities, which could lead to a broader distribution of performance), the data are presented as box plots in Figure 7g−h, with the data grouped into linear mass density ranges of 0.5 tex. Figure 7g−h shows that the strength and stiffness median values decrease with increasing linear mass density for the five data sets, verifying that the strength and stiffness measurably increase as the fiber size decreases.

The inverse relationship between the fiber diameter and both strength and stiffness are observed for fibers prepared using each of the studied densification methods as well as for undensified fibers. Therefore, these relationships may be attributed at least in part to factors that are not overcome by densification, such as the undensified CNT organization and the loading technique. For example, fiber spatial nonuniform-

ities resulting from the growth process, CNT tortuosity, ineffective inter-CNT load transfer, or nonuniform loading of the fiber at the grips can lead to load-bearing in only a fraction of the CNTs within a fiber, which can substantially lower both the strength and stiffness of the fibers. Spatial nonuniformities within the fiber or nonuniform loading at the grips are expected to have contributed to the large spread and scatter in the strength and stiffness data, even for fibers with equivalent linear mass density, because the nonuniformities that can limit the fraction of CNTs within a fiber that are load bearing at a given time will vary between fibers. The effects of nonuniform loading are expected to be more pronounced in larger fibers with higher linear mass densities, resulting in lower strength and stiffness values for the fibers with higher linear mass densities.

The statistics shown in Figure 7g−h are used to quantify the effects of densification on fiber strength and stiffness. Compared with undensified fibers, capillary densification resulted in the highest increase in fiber strength and stiffness. The effect is most pronounced for fibers with small linear mass densities of less than 0.5 N tex^{-1}; on average, capillary densification increased the strength by 80% and the stiffness by 170% as compared with undensified fibers in that range. For mechanically densified fibers with linear mass densities less than 0.5 N tex^{-1}, the strength increased by 15% and the stiffness by 100% on average compared with undensified fibers. The three sets of fibers densified mechanically showed similar performance to one another, with small improvements resulting from the secondary densification technique. Compared with mechanical densification alone in the 0−0.5 tex range, secondary capillary densification increased the mean strength by 7% and the mean stiffness by 11%, whereas twisting increased the mean strength by 24% and decreased the mean stiffness by 47%. The reduction of stiffness resulting from twisting is expected because twisting causes the CNTs to be loaded in tension at an oblique angle with respect to the main fiber axis.[27]

Measuring fiber toughness and fracture zone length provide an additional understanding of fiber performance. Fiber toughness (the energy absorbed by a fiber up until fracture) is plotted as a function of the linear mass density as a box plot in Figure 8. There is a clear inverse relationship between the fiber toughness and the linear mass density: larger fibers require less energy per unit mass to fracture. This effect is attributed to nonuniform loading that becomes more pronounced as fiber size increases, which is similar to the effect seen in the strength and stiffness data. Densification improves fiber toughness for all densification methods. For fibers in the 0−0.5 tex range compared with undensified fibers, the mean toughness increased by 42% for capillary densification, 80% for mechanical densification, 45% for mechanical and capillary densification, and 81% for mechanical densification and twisting.

The fracture-zone lengths of fibers tested in tension to failure using an SEM displacement stage are plotted in Figure 9. The fracture-zone length of a fiber is defined as the length of the region adjacent to a broken end whose appearance differs from the rest of the fiber structure. SEM images of fibers before and after fracture are shown in Figure 3. Short fracture zones are seen in geometrically compact, dense, mechanically densified fibers, whereas capillary-densified fibers and undensified fibers have longer fracture zones. The general trend is that fracture zone length decreases as the fiber density increases, with shorter fracture zones measured in denser fibers and in fibers
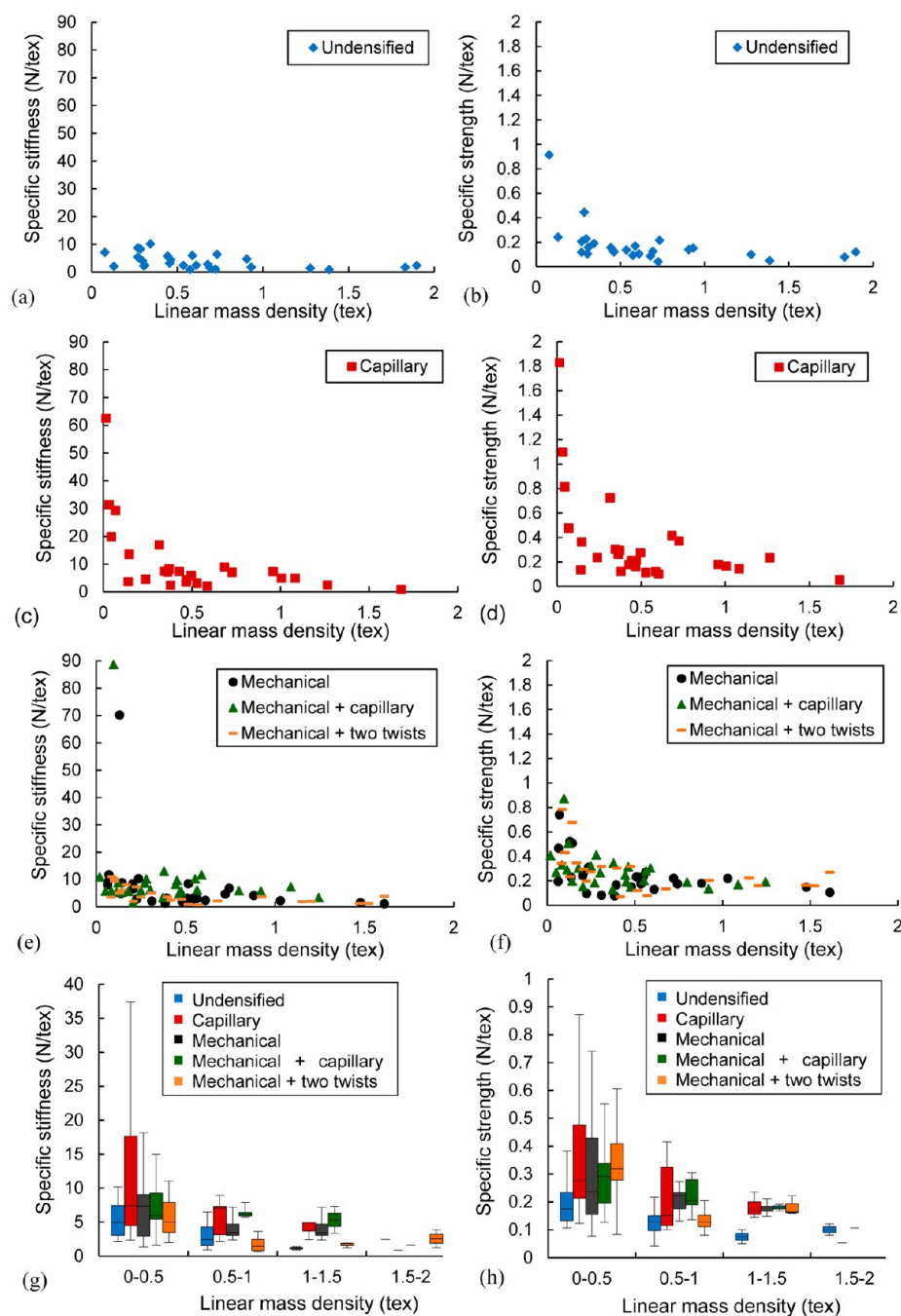
Figure 7. (a) Specific stiffness and (b) specific strength of the undensified fibers; (c) specific stiffness and (d) specific strength of the fibers densified using capillary effects; (e) specific stiffness and (d) specific strength of the fibers densified mechanically with and without secondary densification. The same data in panesl a–f is presented in panels g and h as box plots for the data grouped into linear mass density ranges of 0.5 tex. The boxes display the first quartile, the median, and the third quartile; the lines indicate the lowest data point within 1.5 times the interquartile range of the lower quartile and the highest data point within 1.5 times the interquartile range of the upper quartile.

with smaller maximum lateral extents, although the relatively small number of samples precludes a full statistical analysis. Toughness and fracture-zone length are inversely correlated for these fibers: higher toughness is measured in fibers densified by the methods that result in shorter fracture zones. It is expected that ideal fibers with good alignment, effective and uniform load transfer, and geometrically compact cross sections would have short fracture zones. Long fracture zones, as seen in capillary-densified fibers and undensified fibers, are an indication of poor load transfer across a fiber's cross-section. Note that a short fracture zone can be misleading because dense CNT tangling

and disorder in mechanically densified fibers produced short fracture zones as well, although this occurred at the expense of the high strength and stiffness expected of a high-performance fiber.

The results offer insight into the mechanisms by which densification affects fiber performance. A first effect of densification is to reduce one or both of the fiber's lateral dimensions (e.g., by comparing Figure 3, panels a and e). The resulting, more geometrically compact fibers were expected to improve performance in part because their smaller size and shape could mitigate the effects of uneven fiber loading. Indeed,
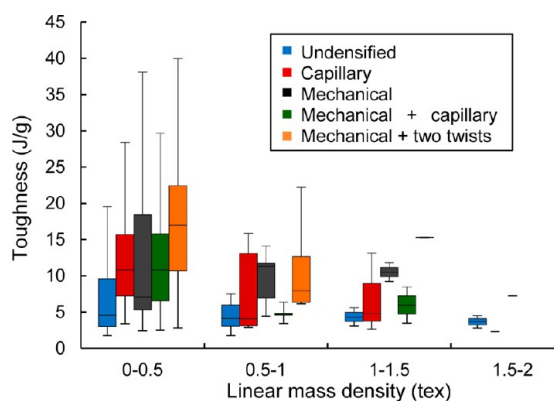
Figure 8. Fiber toughness as a function of linear mass density. The boxes display the first quartile, the median, and the third quartile of fiber toughness; the lines indicate the lowest data point within 1.5 times the interquartile range of the lower quartile and the highest data point within 1.5 times the interquartile range of the upper quartile.

compared with undensified fibers, the data demonstrate an increase in strength, stiffness, and toughness both for the mechanically densified fibers whose lateral dimensions were reduced in both directions compared with their undensified dimensions and for the capillary-densified fibers that formed sheetlike structures with dramatically reduced thickness only. Despite having one large lateral dimension and a long fracture zone, the capillary-densified fibers typically showed greater measured values of strength and stiffness than those densified mechanically. The results indicate that reducing the lateral dimensions does indeed improve performance. Perhaps more importantly, they also demonstrate that the mechanism by which the CNTs densify through self-assembly within capillary densified fibers provides advantages that counteract the presence of uneven loading because of their wide sheetlike structure, enabling strength and stiffness values that are even higher than those of the more compact mechanically densified fibers. Therefore, both the nanoscale CNT interactions and overall fiber cross-sectional shape influence the mechanical properties of the fiber in tension.

A second mechanism by which densification can influence fiber properties and performance is by modifying the interactions among the CNTs in a fiber. Modifying the CNT interactions includes changing the bundle size, increasing the density of contacts between neighboring CNTs and bundles, and changing the degree of CNT alignment along the fiber axis.

Morphological changes within the fibers as a result of densification were studied by imaging the surface of the fibers at high magnification by SEM. As shown in Figure 10, capillary densification causes the CNTs to self-assemble into a densely packed, highly tortuous structure with increased inter-CNT contact and reduced CNT alignment along the fiber axis. Mechanical densification (Figure 10c) results in an increased CNT packing density, increased bundle size, and a greater level of disorder. It is hypothesized that the lower performance in the mechanically densified fibers as compared to capillary-densified fibers may be the result of the less organized nanoscale fiber structure. The higher performance of capillary-densified fibers may be the result of the increased density of inter-CNT contacts produced when CNTs self-assemble into dense, highly contacting networks.

The highest stiffness and strength values for the fibers prepared in this study are 88.7 and 1.8 N tex^{-1}, respectively (Figure 7). The currently achieved values are much lower than the stiffness of an ideal fiber made of parallel SWCNTs (or parallel MWCNTs in which all shells are load bearing), which is 448 N tex^{-1}, assuming an effective SWCNT Young's modulus of 1 TPa. By considering a conservative failure strain of 6%, the ideal strength is 27 N tex^{-1}. The specific strength, specific stiffness, and toughness of the fibers are compared to the tensile properties of state of the art CNT yarns found in the literature and carbon fiber in Table 1. Defects, tortuosity, disorder, imperfect packing, nonuniformities, and the number of CNT walls (because not all walls in a MWCNT are necessarily load bearing) significantly limit the fibers' strength and stiffness. The densification techniques are shown to be able to improve the strength and stiffness of fibers. However, fundamental improvements in the fabrication process, such as making longer, better aligned, and less defective CNTs, will be necessary to enable further improvement in the properties of the macroscopic CNT fibers.

Last, we studied how the densification methods influence the mechanical-energy-storage capacity of the CNT fibers. For this, three sets of fibers (undensified, capillary densified, and mechanically densified) were loaded cyclically in tension. A total of 83 fibers were tested. The applied cyclic strain started at 0.5% and was increased in increments of 0.5% until the fiber fractured. At the maximum applied cyclic strain sustained by each fiber, the area under the stress−strain curve in unloading was integrated to calculate the fiber's extractable stored energy and from that its volumetric energy density (elastic energy
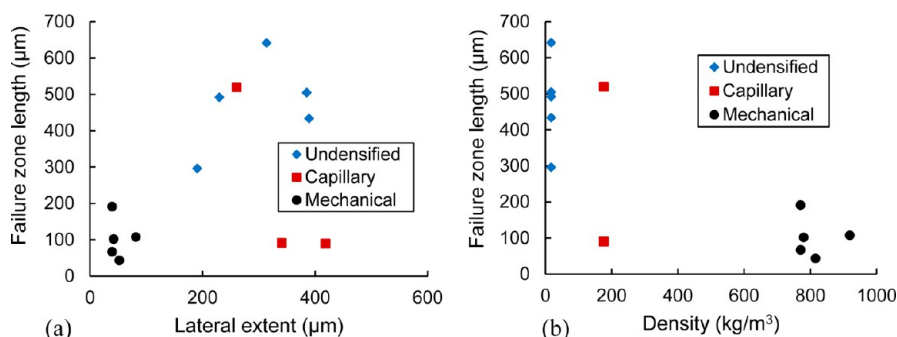

Figure 9. Length of the fracture zone as a function of (a) the maximum lateral extent of the fiber and (b) the fiber density. In panel b, the densities for the undensified and capillary-densified fibers are assumed to be equal to the average density values for fibers densified in that manner. The densities of the mechanically densified fibers described here were not individually measured and are instead estimated from the measured dependence of the density on the linear mass density for mechanically densified fibers (Figure 4).
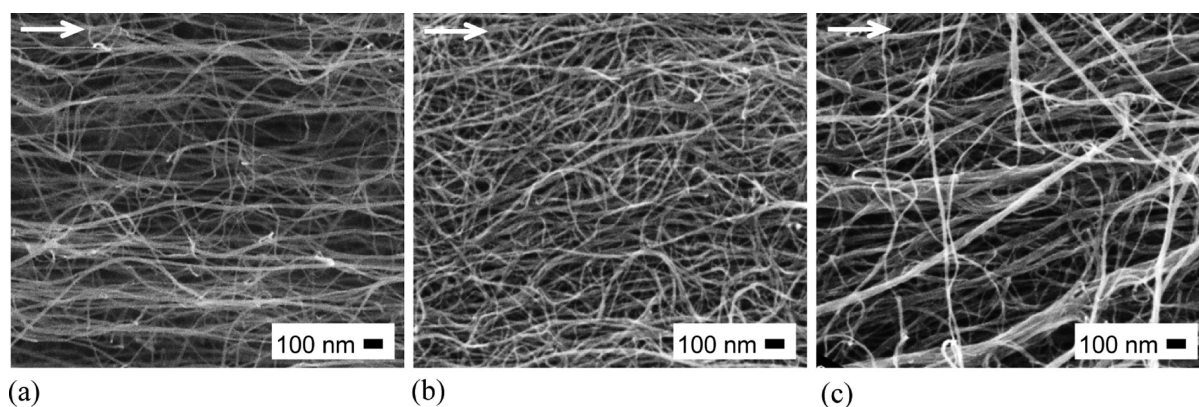
Figure 10. SEM images of CNTs on the surface of fibers prepared with (a) no densification, (b) densification using capillary effects, and (c) mechanical densification. The direction of the fiber axis is indicated with an arrow on each image.

Table 1. Tensile Properties of CNT Fibers, CNTs Yarns, and Carbon Fiber

publication	method	strength	specific strength (N tex^{-1})	Young's modulus (GPa)	specific stiffness (N tex^{-1})	toughness (J/g)
fibers, present work (best values)	fibers from forests	320 MPa	1.8	25	88.7	94
Davis et al.[12]	superacid spinning	50–150 MPa		120		
Behabtu et al.[13]	superacid spinning	1 GPa	0.97	120		
Boncel et al.[28]	dry spinning from aerogel		2.3		75	63
Koziol et al.[6]	dry spinning from aerogel	1.3–8.8 GPa	1.5–9.8	78–357	87–397	13–121
Hill et al.[18]	dry spinning from aerogel	1 GPa	0.86	51.5	44.7	
Zhang et al.[9]	dry spinning from forest	1.35–3.3 GPa		100–263		110–975
ultra-high modulus carbon fiber[29]		3.1 GPa	1.4	966	439	2
high strength carbon fiber[29]		7.1 GPa	3.9	294	162	47

stored per unit volume) and gravimetric energy density (elastic energy stored per unit mass). The volumetric energy density is plotted versus the gravimetric energy density in Figure 11. The wide range of measured gravimetric energy densities is partly attributed to using fibers with a range of linear mass densities, with a higher stored energy per unit mass measured in fibers with smaller linear mass-density values. Because of the greater reduction of their cross section, mechanically densified fibers have the highest volumetric energy density, with a volumetric
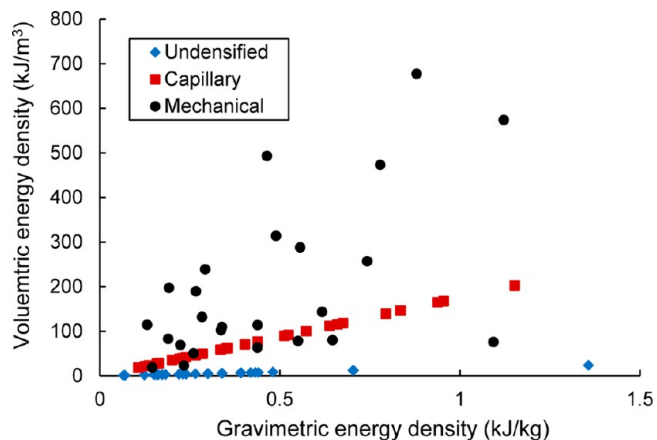

Figure 11. Volumetric energy density as a function of gravimetric energy density for fibers densified using different techniques.

energy density 30 times higher than that of the undensified fibers on average. Because the density of mechanically densified fibers varies between samples and because it is not independent of linear mass density, the relationship between the gravimetric and volumetric energy density for the mechanically densified fibers is not strictly linear.

The overall utility of the methods of densification as a means of increasing the mechanical energy density is evaluated by comparing the fibers' energy densities. Capillary and mechanical densification produced fibers with a more consistently high gravimetric energy density than undensified fibers as a result of their higher strength. The highest energy density measured in these fibers is 1.35 kJ kg^{-1} or 677 kJ m^{-3}. The gravimetric energy density of these fibers, despite their present imperfections, already greatly exceeds the gravimetric energy density of 0.14 kJ kg^{-1} for steel springs, although their volumetric energy density remains below the 1080 kJ m^{-3} value for steel springs.[30] With fabrication improvements, these springs made by loading continuous CNT fibers in tension may be useful to replace small-scale mechanical steel springs for micro- and milli-scale energy-storage applications.[14,18,31]

4. CONCLUSIONS

Continuous fibers made of millimeter-length CNTs serve as a model material to study the mechanical properties of CNT fibers with minimal effects from slip. The results of this study illustrate the challenges of scaling up the properties of individual CNTs into high-performance fibers, namely,

achieving organization of large numbers of CNTs that enables sufficiently uniform loading to take advantage of the stiffness and strength of the individual CNTs. Densification was shown to improve the mechanical properties of CNT fibers in tension by modifying their nanoscale CNT interactions and by reducing their overall cross-sectional dimensions. For the same linear mass density, a higher performance was measured in fibers with reduced lateral extents. Higher strength, stiffness, toughness, and energy density were consistently measured in smaller fibers regardless of the densification method, so nonuniformities are an attribute of the organization of the CNTs in fibers that are amplified in larger fibers and not overcome by densification. Each of the four densification methods consistently produced fibers with higher strength, stiffness, toughness, and energy density than undensified fibers. The highest increases in strength and stiffness were observed in capillary-densified fibers followed by mechanically densified fibers. Capillary densification increases the packing density and intertube interactions through self-assembly and therefore is an effective way to consolidate CNTs to increase fiber performance. Capillary densification without a preferential direction of wicking (to produce densified round fibers rather than flat sheets) has the potential to produce fibers with a smaller lateral extent than the capillary densification used here as well as potentially better performance and should be studied in the future. In situ SEM examination uniquely showed the mechanisms of failure, suggesting that nonuniform CNT load bearing is in large part responsible for the gap between the measured fiber properties and ideal CNT properties. The uniform loading of CNTs in fibers is limited by CNT defects, tortuosity, tangling, fiber spatial nonuniformities resulting from the growth process, and limited interconnections between CNTs that limit inter-CNT load transfer.

The highest strength and stiffness measured in these fibers were 1.8 and 88.7 N tex^{-1}, respectively, and the maximum measured reversible energy density of the fibers was 1.35 kJ kg^{-1} or 677 kJ m^{-3}. The results show that the path to higher performance fibers may lie not only in the use of continuous and long CNTs but also in controlling their density and nanoscale ordering through densification after formation of the initial network, particularly capillary-driven fiber densification. The results from this work highlight the importance of minimizing the introduction of disorder within assemblies of CNTs. Although densification techniques can improve the strength and stiffness of fibers, more fundamental improvements in the CNT fabrication process and its relation to fundamental load-transfer mechanisms are also needed for the properties of CNT fibers to approach the ideal CNT values.

■ AUTHOR INFORMATION

Corresponding Author
*E-mail: fahill@alum.mit.edu.

Notes
The authors declare no competing financial interest.

■ ACKNOWLEDGMENTS

■ REFERENCES

(1) Qian, D.; Wagner, G. J.; Liu, W. K.; Yu, M.; Ruoff, R. S. *Appl. Mech. Rev.* **2002**, *55*, 495−533.
(2) Yu, M.; Files, B. S.; Arepalli, S.; Ruoff, R. S. *Phys. Rev. Lett.* **2000**, *84*, 5552−5555.
(3) Salvetat, J. P.; Bonard, J.; Thomson, N. H.; Kulik, A. J.; Forro, L.; Benoit, W.; Zuppiroli, L. *Appl. Phys. A* **1999**, *69*, 255−260.
(4) Lu, W.; Zu, M.; Byun, J.; Kim, B.; Chou, T. *Adv. Mater.* **2012**, *24*, 1805−1833.
(5) Zhang, X.; Sreekumar, T. V.; Liu, T.; Kumar, S. *J. Phys. Chem. B* **2004**, *108*, 16435−16440.
(6) Koziol, K.; Vilatela, J.; Moisala, A.; Motta, M.; Cunniff, P.; Sennett, M.; Windle, A. H. *Science* **2007**, *318*, 1892−1895.
(7) Li, Y.; Wang, K.; Wei, J.; Gu, Z.; Wang, Z.; Luo, J.; Wu, D. *Carbon* **2005**, *43*, 31−35.
(8) Vilatela, J. J.; Deng, L.; Kinloch, I. A.; Young, R. J.; Windle, A. H. *Carbon* **2011**, *49*, 4149−4158.
(9) Zhang, X.; Li, Q.; Holesinger, T. G.; Arendt, P. N.; Huang, J.; Kirven, P. D.; Clapp, T. G.; DePaula, R. F.; Liao, S.; Zhao, Y.; Zheng, L.; Peterson, D. E.; Zhu, Y. *Adv. Mater.* **2007**, *19*, 4198−4201.
(10) Zhang, M.; Atkinson, K. R.; Baughman, R. H. *Science* **2004**, *306*, 1358−1361.
(11) Zhang, X.; Li, W.; Tu, Y.; Li, Y.; Coulter, J. Y.; Zheng, L.; Zhao, Y.; Jia, Q.; Peterson, D. E.; Zhu, Y. *Small* **2007**, *3*, 244−248.
(12) Davis, V. A.; Nicholas, A.; Parra-Vasquez, G.; Green, M. J.; Rai, P. K.; Behabtu, N.; Prieto, V.; Booker, R. D.; Schmidt, J.; Kesselman, E.; Zhou, W.; Fan, J.; Adams, W. W.; Hauge, R. H.; Fischer, J. E.; Cohen, Y.; Talmon, Y.; Smalley, R. E.; Pasquali, M. *Nat. Nanotechnol.* **2009**, *4*, 830−834.
(13) Behabtu, N.; Young, C. C.; Tsentalovich, D. E.; Kleinerman, O.; Wang, X.; Ma, A. W.; Bengio, E. A.; ter Waarbeek, R. F.; de Jong, J. J.; Hoogerwerf, R. E.; Fairchild, S. B.; Ferguson, J. B.; Maruyama, B.; Kono, J.; Talmon, Y.; Cohen, Y.; Otto, M. J.; Pasquali, M. *Science* **2013**, *339*, 182−186.
(14) Hill, F. A.; Havel, T. F.; Lashmore, D.; Schauer, M.; Livermore, C. *Proceedings of the 11th International Workshop on Micro and Nanotechnology for Power Generation and Energy Conversion Applications*, Seoul, Korea, November 15−18, 2011.
(15) Hill, F. A.; Havel, T. F.; Hart, A. J.; Livermore, C. *J. Micromech. Microeng.* **2009**, 19.
(16) Hill, F. A.; Havel, T. F.; Livermore, C. *Nanotechnology* **2009**, 20.
(17) Hill, F. A.; Havel, T. F.; Hart, A. J.; Livermore, C. *J. Micromech. Microeng.* **2010**, 20.
(18) Hill, F. A.; Havel, T. F.; Lashmore, D. S.; Schauer, M.; Livermore, C. submitted for publication.
(19) Reddy, T. In *Linden's Handbook of Batteries*, 4th ed.; Reddy, T., Linden, D., Eds.; McGraw-Hill Companies: New York, 2011.
(20) Chesnokov, S. A.; Nalimova, V. A.; Rinzler, A. G.; Smalley, R. E.; Fischer, J. E. *Phys. Rev. Lett.* **1999**, *82*, 343−346.
(21) Meshot, E. R.; Plata, D. L; Tawfick, S.; Zhang, Y.; Verploegen, E. A.; Hart, A. J. *ACS Nano* **2009**, *3*, 2477−2486.
(22) Liu, H.; Li, S.; Zhai, J.; Li, H.; Zheng, W.; Jiang, L.; Zhu, D. *Angew. Chem., Int. Ed.* **2004**, *43*, 1146−1149.
(23) Chakrapani, N.; Wei, B.; Carrillo, A.; Ajayan, P. M.; Kane, R. S. *Proc. Natl. Acad. Sci. U.S.A.* **2004**, *101*, 4009−4012.
(24) Fang, S. L.; Zhang, M.; Zakhidov, A. A.; Baughman, R. H. *J. Phys.: Condens. Matter* **2010**, *22*, 33422.
(25) Bedewy, M.; Meshot, E. R.; Reinker, J. J.; Hart, A. J. *ACS Nano* **2011**, *5*, 8974−8989.
(26) Liu, K.; Sun, Y.; Zhou, R.; Zhu, H.; Wang, J.; Liu, L.; Fan, S.; Jiang, K. *Nanotechnology* **2010**, *21*, 045708.
(27) Hearle, J. W., Grosberg, P., Backer. S. *Structural Mechanics of Fibers, Yarns and Fabrics*; John Wiley & Sons: New York, 1969; Vol. 1.
(28) Boncel, S.; Sundaram, R. M.; Windle, A. H.; Koziol, K. K. *ACS Nano* **2011**, *5*, 9339−9344.

(29) Morgan, P. *Carbon Fibers and Their Composites*; Taylor & Francis: Boca Raton, FL, 2005.

(30) Madou, M. *Fundamentals of Microfabrication*; CRC Press: Boca Raton, FL, 2002.

(31) Zhang, Y.; Arnold, D. P. *Sens. Actuators, A* **2012**, *180*, 187−192.